

000 001 002 003 004 005 006 007 008 009 010 011 012 013 014 015 016 017 018 019 020 021 022 023 024 025 026 027 028 029 030 031 032 033 034 035 036 037 038 039 040 041 042 043 044 045 046 047 048 049 050 051 052 053 ARE COLOUR TRAINED MODELS ROBUST IN HANDLING BINARY IMAGES: A FINGERPRINT RECOGNITION STUDY

Anonymous authors

Paper under double-blind review

ABSTRACT

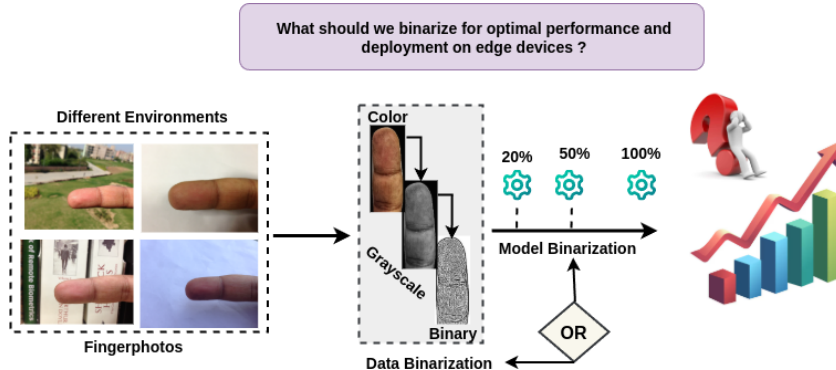
Fingerprint recognition has long been a cornerstone of biometric authentication, yet robust performance across varying imaging conditions remains a challenge, especially fingerphoto, which are generally acquired from the camera, instead of the Livescan images, which are not prone to the environmental factors. Due to the tremendous security demands in large-scale areas and areas where the deployment of computationally heavy devices might not be feasible, like refugee camps, the development of a scalable solution must be a priority. Through this research, we aim to achieve this by understanding the impact of binarization on images and models. Surprisingly, neither the role of Binarized Neural Networks (BNNs) nor binary fingerprint images (especially photos, not scans) has been explored in the literature. Henceforth, in this work, we conduct a comprehensive study of fingerprint recognition using both floating-point-based Deep Neural Networks (DNNs) and Binarisied Neural Networks (BNNs) across multiple image representations, ranging from RGB to grayscale to binary. Our experiments reveal that while DNNs excel with richer representations such as RGB and grayscale, BNNs demonstrate superior compatibility with binary fingerprints, effectively leveraging their reduced complexity to achieve competitive or even better recognition accuracy. This finding highlights the importance of aligning model architectures with input spectra: full-precision networks benefit from information-rich domains, whereas binarized models coupled with binary images offer both efficiency and improved accuracy in inherently discrete representations. The results provide new insights into spectrum-aware fingerprint recognition, guiding the design of accurate and resource-efficient biometric systems.

1 INTRODUCTION

Fingerprint recognition has long served as the cornerstone of biometric authentication due to its uniqueness, permanence, and ease of acquisition. Over decades, research on contact-based fingerprint sensors has delivered highly reliable performance under controlled conditions, enabling deployment in large-scale national identity programs, border management, and consumer-grade authentication systems. However, with the rising demand for contactless biometric solutions—particularly in remote and mobile authentication scenarios—fingerphoto recognition, wherein fingerprints are captured using commodity cameras such as those embedded in smartphones, has emerged as a promising alternative (Donida Labati et al., 2019; Malhotra et al., 2024). This modality offers clear advantages: it is hygienic, cost-effective, and obviates the need for specialized hardware. Yet, fingerphoto recognition introduces several unique challenges arising from unconstrained acquisition: uncontrolled illumination, diverse backgrounds, variations in skin tone, motion blur, and environmental noise (Sreehari & Anzar, 2025).

Unlike contact-based sensors that are engineered to optimise ridge–valley contrast, fingerphotos are captured under consumer-grade imaging pipelines that often involve automatic white-balancing, colour processing, and compression, thereby altering the fingerprint signal. Prior works have shown that domain mismatch between contact and contactless modalities can substantially degrade recognition performance (Grosz et al., 2021). A critical but underexplored aspect of these challenges lies in the spectral representation of fingerphotos, whether they are processed in RGB, grayscale,

054
055
056
057
058
059
060
061
062
063
064
065



066 Figure 1: Can spectrum choice decide whether recognition models succeed or fail? Why do binary
067 models thrive on binary images, while color spectra shift the outcome?

068
069
070
071
072
073
074
075
076
077
078
079
080
081
082
083
or binary form. Traditional fingerprint systems rely primarily on grayscale representations that capture ridge-valley structures and minutiae points, forming the basis of classical fingerprint matching. Fingerphotos, however, inherently capture richer colour information, which may encode additional textural cues useful for recognition (Murshed et al., 2023). Subsequently, being captured from smartphone cameras, which these days are of significantly high resolution, storing these fingerphotos is also creating a serious issue for edge devices. For example, a single fingerphoto image captured from an Android camera provides an image of resolution 3072×4096 and of size 2.51 Mb. One can imagine where millions of identities need to be matched, saving such high storage-demanding images is challenging. On the other hand, binary representations emphasise the ridge structures more explicitly, but at the cost of discarding subtle colour and intensity variations. The choice of spectrum thus directly influences recognition accuracy, model robustness, and computational efficiency. Despite its importance, a systematic study of spectrum-aware fingerphoto recognition, spanning RGB, grayscale, and binary domains, remains largely absent in the existing literature. Due to several challenges involved in the processing of fingerphoto images, especially the cost of storing both heavy model weights (full precision floating points) and images (several of MBs), this research aims to advance fingerphoto recognition for mobile devices including edge-devices.

084
085
086
087
088
089
090
091
092
093
094
095
096
097
098
099
100
With the advent of Deep Neural Networks (DNNs), spectrum-rich representations (RGB and grayscale) can be effectively leveraged for extracting fine-grained intensity, texture, and structural cues. In contrast, Binarized Neural Networks (BNNs), which quantize weights and activations to binary values, cause significant efficiency gains by reducing both memory footprint and computational cost (Zhang et al., 2023). However, their performance often deteriorates when handling high-variance input distributions, such as unconstrained fingerphotos. This raises a fundamental research question: How does the spectral domain of input data impact fingerphoto recognition performance across full-precision and binarized models? Further, the recent study (Zhang et al., 2025) shows that the BNNs are highly robust in handling adversarial corruptions on large-scale datasets than the full precision models. Therefore, utilising the BNNs coupled with binary images will not only save the computational cost but also ensure the developed safety-critical system is robust to adversarial perturbations. In this work, we present the first comprehensive study on spectrum-aware fingerphoto recognition across RGB, grayscale, and binary representations, systematically evaluating the trade-offs between accuracy, efficiency, and generalization (Figure: 1). Our contributions can be summarized as follows: (i) We conduct a systematic evaluation of widely used pretrained DNNs alongside pretrained BNNs, analyzing their recognition performance on fingerphotos represented in color (RGB), grayscale, and binary domains. (ii) We explore mixed-precision architectures by selectively binarizing layers within DNNs trained on color fingerphotos, and examine their impact on recognition accuracy across different spectral domains. This hybrid design highlights a new pathway for balancing accuracy and efficiency in fingerphoto recognition.

103 2 RELATED WORK

104
105
106 The transition from traditional contact-based fingerprint systems to touchless fingerphoto recogni-
107 tion has opened up promising directions for hygienic, cost-effective, and mobile-friendly authenti-
cation. However, it has also introduced unique challenges related to acquisition, spectral represen-

108 tation, and interoperability. Recent surveys highlight that unlike touch-based systems, fingerphotos
 109 are highly susceptible to uncontrolled illumination, background clutter, variations in pose, and scale
 110 distortion, making robust recognition a non-trivial task (Priesnitz et al., 2021; Kaplesh et al., 2025).
 111 These limitations emphasize the need for systematic investigations that go beyond conventional
 112 grayscale ridge–valley matching to fully exploit and evaluate spectral representations. To support
 113 research in this direction, several databases have been introduced. Chopra et al. released one of the
 114 first unconstrained fingerphoto datasets, explicitly capturing variations in illumination, background,
 115 and hand positioning, thereby highlighting the challenges of recognition under real-world conditions
 116 (Chopra et al., 2018). Other efforts such as ISPFDv2 and related collections attempted to capture
 117 semi-controlled fingerphoto images, yet fully unconstrained benchmarks remain scarce. In parallel,
 118 work on preprocessing and interoperability has sought to bridge the gap between contactless
 119 and legacy contact-based systems. Early contributions demonstrated that resolution normalization
 120 and rescaling of fingerphotos toward the 500 dpi standard used in contact sensors improved cross-
 121 domain matching (Kunsuk & Areekul, 2023). Building on this, CNN-based frameworks such as
 122 the multi-Siamese architecture of Lin and Kumar combined ridge and minutiae-based representa-
 123 tions to learn domain-invariant features, significantly enhancing contactless-to-contact recognition
 124 performance (Lin & Kumar, 2018).

125 At the algorithmic level, deep neural networks have been central to recent advances in feature ex-
 126 traction. Tang et al. proposed FingerNet, a unified architecture that integrates fingerprint domain
 127 knowledge, such as orientation estimation, enhancement, and minutiae detection—within an end-to-
 128 end deep network, thereby improving robustness on noisy and latent fingerprints (Tang et al., 2017).
 129 Beyond domain-specific designs, researchers have also investigated whether ImageNet-pretrained
 130 object recognition networks can generalize to biometric tasks. Kumar and Agarwal showed that
 131 such models transfer surprisingly well to modalities including face, iris, and fingerprint, often
 132 providing competitive accuracy without requiring large task-specific datasets (Kumar & Agarwal,
 133 2024). These findings suggest that spectrum-rich fingerphotos, particularly in RGB, could be better
 134 exploited by leveraging pretrained architectures. In parallel, efficiency has become an important
 135 consideration, as fingerphoto recognition is increasingly deployed on mobile devices. Recent devel-
 136 opments in network binarization have shown that Binary Neural Networks (BNNs), which restrict
 137 both weights and activations to binary values, can drastically reduce model size and computational
 138 cost, making them well-suited for deployment on resource-constrained platforms (Qin et al., 2020).
 139 However, such binarization often comes with a drop in recognition accuracy, especially when ap-
 140 plied to high-variance biometric data such as unconstrained fingerphotos. This raises open questions
 141 about how binarized and hybrid architectures perform when exposed to different spectral domains.

142 While prior works have significantly advanced touchless fingerprint recognition in terms of datasets,
 143 preprocessing pipelines, and architectural design, there remains a lack of systematic study on
 144 spectrum-aware fingerphoto recognition. Specifically, the implications of representing fingerpho-
 145 tos in color, grayscale, or binary domains, and how these interact with full-precision deep models
 146 versus binarized networks, remain largely unexplored. In this work, we address this gap by conduct-
 147 ing a comprehensive analysis of fingerphoto recognition across RGB, grayscale, and binary spectra.
 148 We evaluate both pretrained and fine-tuned deep networks, investigate the generalization ability of
 149 spectrum-aware models, and explore mixed-precision architectures that selectively binarize layers
 150 to balance efficiency and accuracy. In doing so, our study provides new insights into the trade-offs
 151 between spectral representation, recognition performance, and computational complexity in finger-
 152 photo recognition.

153 3 EXPERIMENTAL SETUP FOR COST-EFFECTIVE FINGERPHOTO 154 RECOGNITION

155 3.1 FINGERPHOTO DATASETS

156 For our experiments, we employ the IIIT-D SmartPhone Finger-selfie Database v1 (ISPFDv1)
 157 (Sankaran et al., 2015), a fingerphoto dataset collected using smartphones. The database originally
 158 consists of 64 subjects; however, due to missing information for one subject, we utilize data from 63
 159 subjects in our study. For each subject, eight color fingerphotos are available, corresponding to the
 160 right index and right middle fingers. These images are captured under two distinct background con-
 161 ditions, natural and white, across both indoor and outdoor environments, thereby ensuring diversity

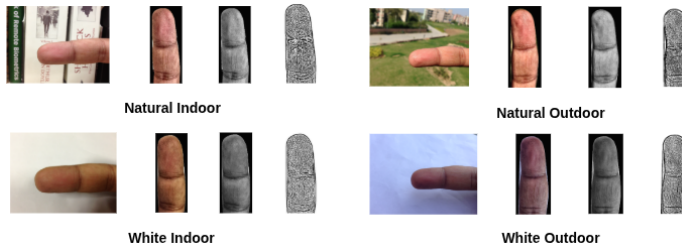


Figure 2: Figure illustrating color, grayscale, and binary fingerphoto images. It reflects the challenges involving illumination and background in fingerphoto recognition. These factors also play a major role when converting images to binary version, hence inaccurate conversion can lead to the poor performance.

in illumination and background variability. The dataset represents four acquisition scenarios: Natural Indoor (NI), Natural Outdoor (NO), White Indoor (WI), and White Outdoor (WO), each having different background conditions. It is interesting to note that livescan images are not only insensitive to illumination, but there is no role of background. Due to these factors, fingerphoto recognition is a complex case than the livescan fingerprint.

To prepare the dataset, we first segment the fingerphoto images and subsequently apply enhancement for further use. The fingerprint region is segmented using the COLFISPROOF method (Kolberg et al., 2023) with a ResNet50 backbone, followed by morphological post-processing, connected component analysis, and convex hull refinement to isolate the largest foreground region. To improve segmentation quality, we additionally generate a version of the fingerphoto with a black background, reapply the COLFISPROOF segmentation, and select the better of the two outputs. The final segmented image is then enhanced using Contrast Limited Adaptive Histogram Equalization (CLAHE) (Zuiderveld, 1994) on the luminance channel in the LAB color space. CLAHE adaptively increases local contrast while avoiding noise amplification, thereby improving ridge-valley visibility in the fingerphotos. These enhanced images are subsequently employed for fingerphoto recognition.

3.2 COLOR-SPACE CONVERSION: RGB-GRAY-BINARY

To normalize the spectral domain of the dataset, we convert RGB fingerphoto images into grayscale using the OpenCV implementation. Specifically, each pixel in the grayscale image is obtained as a weighted sum of the original Red, Green, and Blue channels: $I_{gray} = 0.299R + 0.587G + 0.114B$. This formulation reflects the human visual system's higher sensitivity to green, followed by red and blue, ensuring perceptually consistent brightness preservation during conversion. The process is applied uniformly across all images while maintaining the original folder hierarchy, thereby providing a consistent grayscale dataset for spectrum-aware recognition experiments.

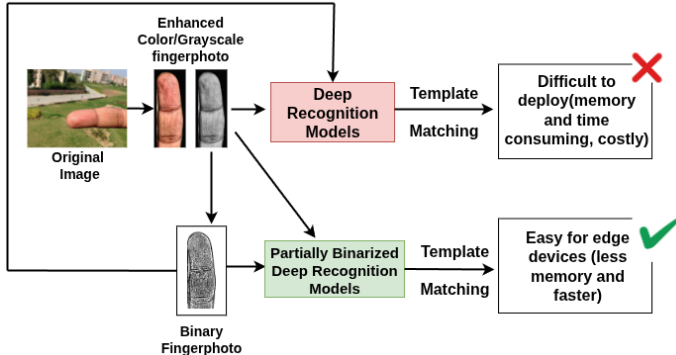
To further normalize the spectrum, grayscale fingerphoto images are converted into binary form using *adaptive Gaussian thresholding* (Rehman & Haroon, 2023). In this approach, each pixel intensity is compared against a locally computed threshold derived from a weighted mean of its neighborhood, adjusted by a constant. Formally, for each pixel $p(x, y)$, the binary value is assigned as

$$B(x, y) = \begin{cases} 255, & \text{if } p(x, y) > T(x, y) - C, \\ 0, & \text{otherwise,} \end{cases} \quad (1)$$

where $T(x, y)$ denotes the Gaussian-weighted mean intensity of a block of size 11×11 centered at (x, y) , and $C = 2$ is a correction factor. This local adaptive method is more robust than global thresholding in handling illumination variations and non-uniform contrasts, thereby preserving ridge structures in the binarized fingerphoto images.

Figure 2 shows the fingerphoto images demonstrating color, grayscale, and binary spectrum, further reflecting the information present in each spectrum.

216
217
218
219
220
221
222
223
224
225
226
227



228
229 Figure 3: Figure illustrating color, grayscale, and binary fingerphoto matching. The results indicate
230 that binary fingerphotos, when combined with partially binarized models, achieve superior recogni-
231 tion compared to conventional DNNs trained on color or grayscale inputs, while simultaneously
232 reducing computational cost and model complexity.

233 3.3 ARCHITECTURES FOR FINGERPHOTO RECOGNITION

234 Since the biometric recognition, including fingerprint recognition, works in a zero-shot setting
235 where testing identities are never seen during training and is inspired by the effectiveness of object
236 recognition models (Kumar & Agarwal, 2024), the proposed research utilised several pre-trained
237 models. In this work, we explore both full-precision and binarized deep learning models for
238 spectrum-aware fingerphoto recognition. On the full-precision side, we consider several widely
239 used architectures, ResNet-50, ResNet-101 (He et al., 2016), ViT-16 (Dosovitskiy et al., 2020),
240 EfficientNet-B2, EfficientNet-B4 (Tan & Le, 2019), and ConvNeXt (Liu et al., 2022), that represent
241 different families of convolutional and transformer-based models with proven success in large-scale
242 image classification. To complement these, we also investigate lightweight binarized networks,
243 specifically BNext-S, BNext-M, and BNext-L (Guo et al., 2022), which quantize weights and activa-
244 tions to binary values, thereby drastically reducing memory usage and computational cost (Figure 3).
245

246 Our study proceeds in two stages.

- 247 • First, we evaluate pretrained models directly on the fingerphoto dataset to establish base-
248 line performance across RGB, grayscale, and binary domains. These models are originally
249 trained on large-scale ImageNet variants, enabling us to assess their generalization capa-
250 bilities when transferred to the biometric domain without task-specific adaptation.
- 251 • The core focus of this work lies in exploring binarization strategies. We analyze the per-
252 formance of fully binarized models (BNext-S, BNext-M, BNext-L) as well as mixed-precision
253 variants, where only selected layers of full-precision DNNs like ResNet and ViT are bina-
254 rized. To fine-tune the partially binarized DNN models, we leverage the Tiny-ImageNet-
255 200 object dataset (Wu et al., 2017). This dataset comprises approximately 1.2 million
256 images distributed across 200 object categories. For our experiments, 500 images per class
257 are used for training, while a separate set of 10,000 images is reserved for validation. The
258 inclusion of Tiny-ImageNet not only provides large-scale object diversity but also enables
259 the DNNs and binarized models to generalize effectively before being adapted for finger-
260 photo recognition.
 - 261 – To partially binarize ResNet-50 and ResNet-101, we replace the last 20% or 50%
262 of convolutional layers with binarized counterparts, while keeping the earlier layers in
263 full precision to preserve low-level representational capacity. In these binarized layers,
264 both the convolutional weights and the input activations are quantized to binary values
265 $\{-1, +1\}$, thereby reducing memory usage and computational overhead. Since the sign
266 function used for binarization is non-differentiable, training is made feasible through
267 the straight-through estimator (STE), which allows approximate gradient flow during
268 backpropagation. To stabilize optimization and avoid loss of accuracy, each binarized
269 convolutional layer is followed by batch normalization (BN) and dropout. This hybrid

270 design enables the network to retain much of the expressive power of the original full-
 271 precision ResNet while benefiting from the efficiency gains of binarization, making it
 272 well-suited for spectrum-aware fingerphoto recognition under resource constraints.

273 – To make BinaryViT, the last 20% or 50% of transformer layers are binarized to re-
 274 duce computational complexity while retaining discriminative power. For each binary
 275 linear projection, the weight matrix is quantized as

277 $\mathbf{W}_b = \text{sign}(\mathbf{W}), \quad \mathbf{W}_b \in \{-1, +1\}^{d_{\text{out}} \times d_{\text{in}}},$ (2)

278 while the affine-normalized input is defined as

280 $\mathbf{x}' = \alpha \mathbf{x} + \beta,$ (3)

282 , where α , and β are the affine transformation parameter initially taken as 1 and 0
 283 respectively.

284 and the binary projection is expressed as

285 $\mathbf{y} = \mathbf{x}' \mathbf{W}_b + \mathbf{b}.$ (4)

287 In the self-attention module, binary projections are applied to the queries, keys, and
 288 values:

289 $Q = \mathbf{X} \mathbf{W}_Q^b, \quad K = \mathbf{X} \mathbf{W}_K^b, \quad V = \mathbf{X} \mathbf{W}_V^b,$ (5)

291 with the attention update computed as

293 $\text{Attention}(\mathbf{X}) = \text{softmax} \left(\frac{QK^\top}{\sqrt{d_k}} \right) V.$ (6)

295 In the feed-forward pyramid MLP, the forward pass is expressed as

297 $\mathbf{H}_1 = \sigma(\mathbf{X} \mathbf{W}_1^b), \quad \mathbf{H}_p = f_{\text{pyramid}}(\mathbf{H}_1), \quad \mathbf{Y} = (\mathbf{H}_1 + \mathbf{H}_p) \mathbf{W}_2^b,$ (7)

299 where $f_{\text{pyramid}}(\cdot)$ denotes the multi-scale convolutional aggregation. By binarizing
 300 $\mathbf{W}_Q, \mathbf{W}_K, \mathbf{W}_V, \mathbf{W}_1, \mathbf{W}_2$ while retaining full-precision normalization and residual
 301 paths, BinaryViT significantly reduces FLOPs and memory footprint, yet preserves
 302 recognition accuracy through affine scaling and residual compensation.

303 By systematically comparing pretrained models, fine-tuned models, and binarized models, we pro-
 304 vide a comprehensive evaluation of how spectrum-aware representations interact with network pre-
 305 cision in fingerphoto recognition.

307 4 FINGERPHOTO RECOGNITION RESULTS AND ANALYSIS

309 4.1 EFFECTIVENESS EVALUATION OF PRETRAINED DEEP AND BINARIZED MODELS

311 This study emphasizes the central question of whether color information plays a significant role
 312 in fingerphoto recognition. As shown in Table 1, when color fingerphoto images are evaluated
 313 using color-trained floating-point models such as ResNet-50 in the natural indoor (NI) scenario, the
 314 performance reaches 85.98% under both cosine and Euclidean similarity measures. Comparable
 315 results are observed with other architectures, where ResNet-101 achieves 82.80% and ViT attains
 316 84.13% under the same conditions. Similar trends extend across the natural outdoor (NO), white
 317 indoor (WI), and white outdoor (WO) scenarios. For example, in the NO setting, ResNet-50 and ViT
 318 obtain accuracies of 85.18% and 75.40%, respectively, highlighting the consistent effectiveness of
 319 color images when used with conventional deep neural networks (DNNs). Interestingly, pretrained
 320 binary-weighted networks also demonstrate strong recognition performance on color fingerphotos.
 321 For instance, BNext-T achieves 82.80% and BNext-S yields 83.60% in NI, which are competitive
 322 with their floating-point counterparts. This trend is consistent across other acquisition scenarios,
 323 suggesting that color images provide sufficient discriminative cues regardless of whether they are
 324 processed by full-precision or binarized models. In other words, color representations appear to be
 325 robust to the underlying network precision, consistently producing compatible performance.

324	Scenario	Spectrum	Metric	ResNet50	ResNet101	ViT	EffNet-B2	EffNet-B4	ConvNeXt-T	BNext-T	BNext-S	BNext-M	BNext-L
325	NI	Grayscale	Color	85.98	82.80	84.13	80.16	69.58	73.28	82.80	83.60	82.80	78.04
326			Euc	85.98	82.28	82.28	80.95	68.52	73.02	83.33	83.86	82.54	77.51
327			Cos	83.07	81.75	82.28	78.31	83.60	80.42	80.42	82.80	79.89	81.75
328		Binary	Euc	83.07	80.69	80.42	78.31	84.13	82.01	80.16	83.60	80.42	80.42
329			Cos	62.96	59.52	60.32	61.38	64.29	69.05	65.61	70.90	70.37	67.99
330			Euc	61.90	58.73	61.11	61.64	62.96	68.78	65.08	70.63	70.11	68.25
331	NO	Grayscale	Color	85.18	85.18	75.40	78.83	79.63	83.07	82.80	82.54	79.89	77.25
332			Euc	84.13	84.13	73.01	78.04	79.10	83.07	83.07	82.01	79.1	76.45
333			Cos	84.92	80.95	72.75	82.54	80.69	80.16	84.92	82.80	82.54	81.22
334		Binary	Euc	84.66	79.89	70.90	82.01	80.16	80.95	84.39	82.54	82.27	81.75
335			Cos	64.55	66.66	53.97	69.57	69.05	71.69	70.37	73.81	70.37	69.58
336			Euc	62.96	66.14	53.17	70.10	66.93	70.90	70.63	74.07	70.63	69.05
337	WI	Grayscale	Color	72.22	73.54	71.16	69.58	77.51	72.22	68.52	67.99	70.10	70.90
338			Euc	70.90	71.95	70.37	70.63	76.72	71.43	68.78	67.46	70.37	71.16
339			Cos	70.37	68.78	72.49	71.43	71.96	71.96	67.19	68.78	67.19	65.34
340		Binary	Euc	70.37	67.19	71.43	70.37	72.22	71.69	67.19	69.84	67.46	65.61
341			Cos	50.79	52.64	48.94	48.94	53.97	52.38	52.64	52.38	52.64	44.44
342			Euc	49.20	52.64	48.41	48.15	53.97	52.91	51.85	53.17	53.70	43.65
343	WO	Grayscale	Color	70.63	71.43	61.64	67.72	69.58	73.28	71.43	73.28	73.54	60.32
344			Euc	65.87	70.90	61.11	66.4	68.62	73.01	71.69	73.28	74.07	60.05
345			Cos	67.19	68.78	60.58	70.37	71.16	71.43	70.9	73.81	72.22	69.58
346		Binary	Euc	63.49	69.05	58.20	70.10	70.37	73.28	69.84	74.34	72.49	69.31
347			Cos	53.17	55.29	48.15	61.37	61.11	60.85	52.64	57.94	55.82	54.50
348			Euc	53.17	53.97	48.15	59.52	60.32	60.32	51.85	57.41	56.08	55.55

Table 1: Performance comparison (Top-1 accuracy in %) across four scenarios (Natural Indoor, Natural Outdoor, White Indoor, White Outdoor), three spectral domains (Color, Grayscale, Binary), and two distance/similarity metrics (Cosine, Euclidean). Models are shown as columns.

351	Scenario	Model	Fraction of Binarization	Color		Grayscale		Binary		
				Cos	Euc	Cos	Euc	Cos	Euc	
352	NI		20%	80.42	78.84	82.54	78.57	17.46	17.20	
353			50%	79.89	77.25	80.95	80.16	22.75	20.90	
354	NO	ResNet101	20%	78.04	75.40	76.72	75.93	21.43	17.72	
355			50%	81.48	77.51	73.28	74.34	20.63	21.96	
356	WI		20%	73.02	68.25	67.72	64.29	17.20	15.87	
357			50%	66.40	64.29	65.87	61.38	19.58	21.43	
358	WO		20%	69.31	67.72	66.93	65.87	15.61	14.55	
359			50%	68.25	68.52	62.70	62.96	20.90	17.46	

Table 2: Performance comparison (Top-1 accuracy in %) across four scenarios (Natural Indoor, Natural Outdoor, White Indoor, White Outdoor), three spectral domains (Color, Grayscale, Binary), and two similarity measures (Cosine, Euclidean) for partially binarized ResNet101 (20% and 50% layers). Best values in each row are highlighted in bold.

In contrast, binary fingerphoto representations reveal a different and more nuanced relationship with network architectures. While floating-point models such as ResNet-50 achieve at most 60.96% accuracy on binary images, binarized models exhibit notably higher performance. For example, in NI, BNext variants achieve between 60.96% and 70.59%, clearly surpassing the floating-point baselines. This effect is even more pronounced in the NO setting, where BNext-S attains 73.81%, representing nearly a 9% improvement over ResNet-50. Similar relative gains are also observed in the WI and WO scenarios. These results lead to two key insights. First, color fingerphotos retain discriminative information that enables consistent recognition performance across both floating-point and binarized networks. Second, binary fingerphotos align better with binarized models, where the compatibility between binary input distributions and binary network weights yields superior recognition accuracy compared to their floating-point counterparts. Together, these findings highlight that while color remains a strong and versatile representation, binary fingerphotos can be more efficiently and effectively recognized by binarized architectures, offering a unique advantage in resource-constrained biometric systems.

378
379

4.2 PERFORMANCE TRENDS IN PARTIALLY BINARIZED NETWORKS

380

381 Based on the results in Table 2, we propose the use of partially binarized deep neural networks
 382 (DNNs) to systematically examine the dependency of binary fingerphoto representations on network
 383 architecture. The analysis reveals distinct trends across spectral domains. For color inputs, we
 384 observe that increasing the proportion of binarized layers in a floating-point model generally leads
 385 to a decline in recognition performance. For example, when color fingerphotos are processed by
 386 ResNet-101 with 20% of its layers binarized, the performance is 80.42%, whereas this drops to
 387 79.89% when 50% of the layers are binarized. A more pronounced decrease is observed in the white
 388 indoor (WI) scenario, where the performance falls from 73.02% (20% binarized) to 66.40% (50%
 389 binarized). These results suggest that color and grayscale fingerphotos, which carry richer spectral
 390 and textural cues, are better recognized by models that retain a larger fraction of floating-point
 391 precision, as binarization reduces the network’s ability to preserve fine-grained intensity variations.

392

393 Interestingly, the opposite trend is observed for binary fingerphotos. Unlike color or grayscale im-
 394 ages, binary representations consist primarily of discrete ridge–valley structures, which align more
 395 naturally with the quantized decision boundaries of binarized networks. For instance, in the NI
 396 scenario, recognition accuracy with ResNet-101 improves from 17.46% with 20% binarization to
 397 22.75% with 50% binarization. Similarly, in the WI scenario under Euclidean distance, performance
 398 increases from 15.87% (20%) to 21.43% (50%). These results indicate that as the binarization level
 399 in the model increases, the network becomes more compatible with the binary input distribution,
 400 yielding improved performance. Taken together, these findings highlight a complementary relation-
 401 ship between image representation and network architecture. While color and grayscale fingerphotos
 402 benefit from models that retain higher floating-point precision, binary fingerphotos exhibit stronger
 403 affinity with highly binarized models. This dual behavior underscores the importance of spectrum-
 404 aware model design: the optimal degree of binarization should be carefully chosen depending on
 405 whether the input images are represented in color, grayscale, or binary form.

406

407

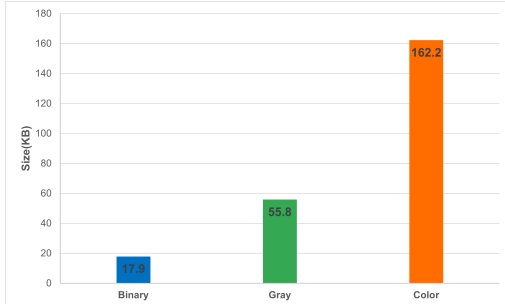
4.3 EFFICIENCY ANALYSIS: IMAGE AND MODEL SIZES

408

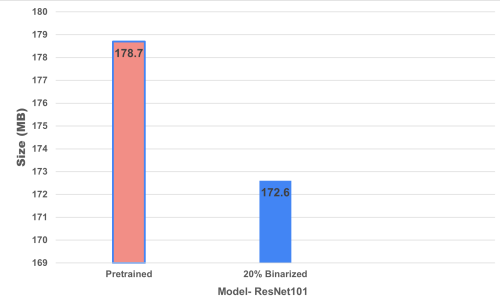
409 In addition to recognition, we analyse the storage efficiency of different spectral representations
 410 and model architectures. The results in Figure 4a show that binary fingerphoto images occupy
 411 substantially less storage compared to grayscale and color counterparts, making them more suitable
 412 for resource-constrained environments. A similar trend is observed for models, where partially
 413 binarized ResNet variants require less storage than their full-precision pretrained counterparts as
 414 shown in Figure 4b. These findings demonstrate the effectiveness of binarization in reducing both
 415 data and model size.

416

417

418
419
420
421
422
423
424
425

(a) Comparison of fingerphoto image sizes (Color, Grayscale, Binary).



(b) Comparison of model sizes (Pretrained vs. partially binarized).

426

427

Figure 4: Storage and model size analysis. Binary fingerphoto images and partially binarized models
 require significantly less storage compared to their full counterparts.

428
429
430
431

432 4.4 LIMITATIONS AND FUTURE SCOPE
433434 The dataset contains illumination variations that can affect binary fingerphoto conversion and reduce
435 recognition accuracy. Future work can explore illumination-invariant preprocessing and more robust
436 models.437 438 5 DISCUSSION AND CONCLUSION
439440 This study systematically examined fingerphoto recognition across different spectral representations,
441 RGB, grayscale, and binary, using both floating-point-weights-based deep neural networks (DNNs)
442 and binarised neural networks (BNNs). The results demonstrate a clear spectrum-dependent be-
443 haviour: full-precision DNNs achieve the best performance when processing information-rich inputs
444 such as RGB and grayscale fingerphotos, while BNNs exhibit a stronger affinity with binary images,
445 where the discrete ridge–valley structures align naturally with their quantized representations. Be-
446 yond recognition accuracy, we also observe significant efficiency advantages. Binary images require
447 substantially less storage compared to grayscale and color images, and partially binarized models
448 are consistently smaller in size than their full-precision counterparts. These findings emphasize
449 the importance of spectrum-aware model selection and architecture design: full-precision networks
450 are more effective in information-rich domains, whereas binarized networks not only achieve bet-
451 ter alignment with binary inputs but also reduce storage and computational demands. Overall, this
452 work provides valuable insights into the design of fingerprint recognition systems that balance ac-
453 curacy, efficiency, and scalability, enabling robust deployment in real-world, mobile, and resource-
454 constrained environments. We believe the presence of such a first-ever understanding can advance
455 the deployment of fingerphoto recognition, especially for remote areas where high computational
456 cost is still infeasible and secure the identities in refugee camps.457 REFERENCES
458459 Shaan Chopra, Aakarsh Malhotra, Mayank Vatsa, and Richa Singh. Unconstrained fingerphoto
460 database. In *Proceedings of the IEEE Conference on computer vision and pattern recognition*
461 workshops, pp. 517–525, 2018.462 Ruggero Donida Labati, Angelo Genovese, Vincenzo Piuri, and Fabio Scotti. A scheme for fin-
463 gerphoto recognition in smartphones. *Selfie Biometrics: Advances and Challenges*, pp. 49–66,
464 2019.466 Alexey Dosovitskiy, Lucas Beyer, Alexander Kolesnikov, Dirk Weissenborn, Xiaohua Zhai, Thomas
467 Unterthiner, Mostafa Dehghani, Matthias Minderer, Georg Heigold, Sylvain Gelly, et al. An
468 image is worth 16x16 words: Transformers for image recognition at scale. *arXiv preprint*
469 *arXiv:2010.11929*, 2020.470 Steven A Grossz, Joshua J Engelsma, Eryun Liu, and Anil K Jain. C2cl: Contact to contactless
471 fingerprint matching. *IEEE Transactions on Information Forensics and Security*, 17:196–210,
472 2021.474 Nianhui Guo, Joseph Bethge, Christoph Meinel, and Haojin Yang. Join the high accuracy club on
475 imagenet with a binary neural network ticket. *arXiv preprint arXiv:2211.12933*, 2022.477 Kaiming He, Xiangyu Zhang, Shaoqing Ren, and Jian Sun. Deep residual learning for image recog-
478 nition. In *Proceedings of the IEEE conference on computer vision and pattern recognition*, pp.
479 770–778, 2016.480 Pooja Kaplesh, Aastha Gupta, Divya Bansal, Sanjeev Sofat, and Ajay Mittal. A systematic review of
481 end-to-end framework for contactless fingerprint recognition: Techniques, challenges, and future
482 directions. *Engineering Applications of Artificial Intelligence*, 150:110493, 2025.484 Jascha Kolberg, Jannis Priesnitz, Christian Rathgeb, and Christoph Busch. Colfispoof: A new
485 database for contactless fingerprint presentation attack detection research. In *Proceedings of the*
IEEE/CVF Winter Conference on Applications of Computer Vision, pp. 653–661, 2023.

486 Vishesh Kumar and Akshay Agarwal. Are object recognition models effective and unbiased for
 487 biometric recognition? In *2024 IEEE International Joint Conference on Biometrics (IJCB)*, pp.
 488 1–10, 2024. doi: 10.1109/IJCB62174.2024.10744463.

489 Siwakun Kunsuk and Vutipong Areekul. Finger photo rescaling for interoperability of touchless
 490 and touch-based fingerprint verification. In *2023 17th International Conference on Signal-Image
 491 Technology & Internet-Based Systems (SITIS)*, pp. 168–175. IEEE, 2023.

492 Chenhao Lin and Ajay Kumar. A cnn-based framework for comparison of contactless to contact-
 493 based fingerprints. *IEEE Transactions on Information Forensics and Security*, 14(3):662–676,
 494 2018.

495 Zhuang Liu, Hanzi Mao, Chao-Yuan Wu, Christoph Feichtenhofer, Trevor Darrell, and Saining Xie.
 496 A convnet for the 2020s. In *Proceedings of the IEEE/CVF conference on computer vision and
 497 pattern recognition*, pp. 11976–11986, 2022.

498 Aakarsh Malhotra, Mayank Vatsa, and Richa Singh. *Learning algorithms for multi-tasks of uncon-
 499 strained fingerprint recognition*. PhD thesis, IIIT-Delhi, 2024.

500 MG Murshed, Syed Konain Abbas, Sandip Purnapatra, Daqing Hou, and Faraz Hussain. Deep
 501 learning-based approaches for contactless fingerprints segmentation and extraction. *arXiv
 502 preprint arXiv:2311.15163*, 2023.

503 Jannis Priesnitz, Christian Rathgeb, Nicolas Buchmann, Christoph Busch, and Marian Margraf.
 504 An overview of touchless 2d fingerprint recognition. *EURASIP Journal on Image and Video
 505 Processing*, 2021(1):8, 2021.

506 Haotong Qin, Ruihao Gong, Xianglong Liu, Xiao Bai, Jingkuan Song, and Nicu Sebe. Binary neural
 507 networks: A survey. *Pattern Recognition*, 105:107281, 2020.

508 Nehal Abdul Rehman and Farah Haroon. Adaptive gaussian and double thresholding for contour
 509 detection and character recognition of two-dimensional area using computer vision. *Engineering
 510 Proceedings*, 32(1):23, 2023.

511 Anush Sankaran, Aakarsh Malhotra, Apoorva Mittal, Mayank Vatsa, and Richa Singh. On smart-
 512 phone camera based fingerphoto authentication. In *2015 IEEE 7th International Conference on
 513 Biometrics Theory, Applications and Systems (BTAS)*, pp. 1–7, 2015. doi: 10.1109/BTAS.2015.
 514 7358782.

515 S Sreehari and SM Anzar. Touchless fingerprint recognition: A survey of recent developments and
 516 challenges. *Computers and Electrical Engineering*, 122:109894, 2025.

517 Mingxing Tan and Quoc Le. Efficientnet: Rethinking model scaling for convolutional neural net-
 518 works. In *International conference on machine learning*, pp. 6105–6114. PMLR, 2019.

519 Yao Tang, Fei Gao, Jufu Feng, and Yuhang Liu. Fingernet: An unified deep network for fingerprint
 520 minutiae extraction. In *2017 IEEE International Joint Conference on Biometrics (IJCB)*, pp.
 521 108–116, 2017. doi: 10.1109/BTAS.2017.8272688.

522 Jiayu Wu, Qixiang Zhang, and Guoxi Xu. Tiny imagenet challenge. *Technical report*, 2017.

523 Baochang Zhang, Sheng Xu, Mingbao Lin, Tiancheng Wang, and David Doermann. *Binary Neural
 524 Networks: Algorithms, Architectures, and Applications*. CRC Press, 2023.

525 Jiehua Zhang, Peng Zhao, Li Liu, Bowen Peng, Zhen Liu, Longguang Wang, and Yingmei Wei.
 526 Arbibench: Benchmarking and analyzing adversarial robustness of binarized convolutional neural
 527 networks. *IEEE Transactions on Information Forensics and Security*, 2025.

528 Karel Zuiderveld. Contrast limited adaptive histogram equalization. In *Graphics gems IV*, pp. 474–
 529 485. 1994.

530

531

532

533

534

535

536

537

538

539